Global Change Biology

Global Change Biology (2017) **23**, 840–856, doi: 10.1111/gcb.13444

# Modeled ecohydrological responses to climate change at seven small watersheds in the northeastern United States

AFSHIN POURMOKHTARIAN[1], CHARLES T. DRISCOLL[1], JOHN L. CAMPBELL[2], KATHARINE HAYHOE[3], ANNE M. K. STONER[3], MARY BETH ADAMS[4], DOUGLAS BURNS[5], IVAN FERNANDEZ[6], MYRON J. MITCHELL[7] and JAMES B. SHANLEY[8]

[1]*Department of Civil and Environmental Engineering, Syracuse University, Syracuse, NY 13244, USA,* [2]*US Forest Service, Northern Research Station, Durham, NH 03824, USA,* [3]*Climate Science Center, Texas Tech University, Lubbock, TX 79409, USA,* [4]*Forest Service, Northern Research Station, Morgantown, WV 26505, USA,* [5]*US Geological Survey, Troy, NY 12180, USA,* [6]*School of Forest Resources and Climate Change Institute, University of Maine, Orono, ME 04469-5722, USA,* [7]*Department of Environmental Resources Engineering, SUNY-ESF, Syracuse, NY 13210, USA,* [8]*US Geological Survey, Montpelier, VT 05601, USA*

## Abstract

A cross-site analysis was conducted on seven diverse, forested watersheds in the northeastern United States to evaluate hydrological responses (evapotranspiration, soil moisture, seasonal and annual streamflow, and water stress) to projections of future climate. We used output from four atmosphere–ocean general circulation models (AOGCMs; CCSM4, HadGEM2-CC, MIROC5, and MRI-CGCM3) included in Phase 5 of the Coupled Model Intercomparison Project, coupled with two Representative Concentration Pathways (RCP 8.5 and 4.5). The coarse resolution AOGCMs outputs were statistically downscaled using an asynchronous regional regression model to provide finer resolution future climate projections as inputs to the deterministic dynamic ecosystem model PnET-BGC. Simulation results indicated that projected warmer temperatures and longer growing seasons in the northeastern United States are anticipated to increase evapotranspiration across all sites, although invoking $CO_2$ effects on vegetation (growth enhancement and increases in water use efficiency (WUE)) diminish this response. The model showed enhanced evapotranspiration resulted in drier growing season conditions across all sites and all scenarios in the future. Spruce-fir conifer forests have a lower optimum temperature for photosynthesis, making them more susceptible to temperature stress than more tolerant hardwood species, potentially giving hardwoods a competitive advantage in the future. However, some hardwood forests are projected to experience seasonal water stress, despite anticipated increases in precipitation, due to the higher temperatures, earlier loss of snow packs, longer growing seasons, and associated water deficits. Considering future $CO_2$ effects on WUE in the model alleviated water stress across all sites. Modeled streamflow responses were highly variable, with some sites showing significant increases in annual water yield, while others showed decreases. This variability in streamflow responses poses a challenge to water resource management in the northeastern United States. Our analyses suggest that dominant vegetation type and soil type are important attributes in determining future hydrological responses to climate change.

*Keywords:* climate change, CMIP5, ecohydrology, ecosystem modeling, northeastern United States, water stress, water use efficiency, watershed

*Received 20 April 2016 and accepted 13 June 2016*

## Introduction

Small watersheds are hydrologically distinct landscape units. Streams that drain watersheds provide an integrated signal of ecosystem function. Therefore, stream water at gauged watersheds can be used to evaluate disturbance in upland terrestrial ecosystems. Climate change is expected to alter many physical and biological processes in forest ecosystems, which may in turn influence the supply and temporal distribution of water that flows to downstream rivers and estuaries (Stewart *et al.*, 2005; Hayhoe *et al.*, 2007). Because of the potential for this perturbation to affect water resources in the northeastern United States and elsewhere, assessing the effects of climate change on hydrological processes is critically important.

Climate projections from coupled atmosphere–ocean general circulation models (AOGCMs) suggest that across the northeastern United States, annual average air temperature and precipitation will continue to increase during the 21st Century (NECIA, 2006; Hayhoe *et al.*, 2007; Melillo *et al.*, 2014). Increases in precipitation should result in more available water for

Correspondence: Afshin Pourmokhtarian, tel. + 617 358 0261, fax + 617 353 8399, e-mail: afshin.pourmokhtarian@gmail.com

runoff and evaporation. Warmer temperatures will cause snow to melt earlier and the peak of the snow melt hydrograph to shift earlier in spring (4–5 days over 2010–2039) causing increases in soil moisture and runoff in late winter and early spring (NECIA, 2006). With an extended growing season, soil moisture will decrease in late summer and early fall due to higher evapotranspiration. It is anticipated that increases in precipitation may not be able to compensate for this increase in evapotranspiration, causing a greater probability for seasonal drought (NECIA, 2006; Campbell *et al*., 2009; Pourmokhtarian *et al*., 2012; Melillo *et al*., 2014). These effects are projected to be more pronounced under higher $CO_2$ emissions scenarios compared to lower emissions scenarios, highlighting the important effects of temperature on the hydrological cycle in the northeastern United States (NECIA, 2006; Melillo *et al*., 2014). Climate change is projected to continue across the northeastern United States (NECIA, 2006; Melillo *et al*., 2014) potentially altering ecosystem services, the economy, and the quality of life. Although the impacts of climate change are already evident on United States ecosystems, predictions of the relative importance of these changes and magnitude are highly variable over time and space (Melillo *et al*., 2014).

The spatial and temporal variability and dynamics of climate change challenge our ability to generalize the effects of long-term climatic shifts for any given region. To assess the potential impacts of climate change on forested ecosystems and headwater streams that drain them, a multifaceted approach is required that is capable of resolving multiple climatic drivers (e.g., temperature, precipitation quantity, and distribution) and other anthropogenic stressors likely to simultaneously affect ecosystems over the coming decades. Modeling is a practical approach to probe how future changes in climate may interact with other global change drivers, such as atmospheric deposition, land disturbance, and increasing concentrations of atmospheric $CO_2$ over broad regions. Several studies in the northeastern United States have used physically based rainfall-runoff models to evaluate effects of changing temperature and precipitation on hydrology (e.g., Matonse *et al*., 2011, 2012; Fan *et al*., 2014; Demaria *et al*., 2016). However, these models do not consider the role of vegetation on hydrology, including the effects of higher atmospheric $CO_2$ concentrations on stomatal conductance and fertilization. Therefore, dynamic watershed models that incorporate the role of vegetation such as leaf physiology, changes in leaf area index (LAI), soil moisture availability, foliar N concentrations, carbon allocation, and biomass production on hydrology are pivotal tools to help understand the long-term effects of climate change on water resources.

In this study, we evaluated hydrological responses to climate change at seven small forested watersheds that have been monitored intensively for decades. The watersheds represent a range of climatic conditions, historical land disturbance (e.g., harvesting, fires, ice storms), and biophysical characteristics (e.g., latitude, longitude, elevation, forest type, soil type). All watersheds have mature second-growth forests. The effect of climate change on the hydrology at these watersheds was assessed using PnET-BGC, a forest–soil–water model that simulates water, energy, and element fluxes at the small watershed scale (Gbondo-Tugbawa *et al*., 2001). The overarching goal of our study was to better understand the variability of climate change effects on forested watershed hydrology in the northeastern United States.

## Materials and methods

### *Study sites*

Seven forested watersheds in the northeastern United States with relatively long-term (14–45 years) and comprehensive measurements of vegetation, soils, meteorology, hydrology, and biogeochemistry were selected for this study (Fig. 1; Table 1). These data are important for model parameterization and testing. The study watersheds include the Hubbard Brook Experimental Forest (HBEF) and Cone Pond Watershed (CPW) in the White Mountains, New Hampshire; Bear Brook Watershed in Maine (BBWM) in Maine; Sleepers River Watershed (SRW) in Vermont; Biscuit Brook (BSB) in the Catskill Mountains, New York; Archer Creek in the Huntington Wildlife Forest (HWF) in the Adirondack Mountains, New York; and the Fernow Experimental Forest (FEF) in the Allegheny Mountains, West Virginia (Fig. 1). The selected study sites are all small to midsized, relatively undisturbed mid- to high-elevation watersheds that represent different forest ecosystem types (northern hardwoods, spruce-fir, central hardwoods) and encompass a range of climate, atmospheric deposition, soil conditions, and historical land disturbance. These small, gauged watersheds as the units of study provide an opportunity to quantify hydrological fluxes to evaluate the effects of climate change on watershed hydrology. Brief descriptions of the study sites are provided in supplemental materials and summarized in Table 1.

### *PnET-BGC model*

PnET-BGC is a deterministic dynamic ecosystem model that includes physiological and biogeochemical processes and uses generalized empirical relationships among water, nitrogen, and carbon. It was developed by linking a forest–soil–water model PnET-CN (Aber *et al*., 1997), with a biogeochemical cycling submodel BGC (Gbondo-Tugbawa *et al*., 2001). Through this coupling, PnET-BGC accounts for both water and N limitations on forest productivity. A strength of this model is its ability to simultaneously simulate fluxes of

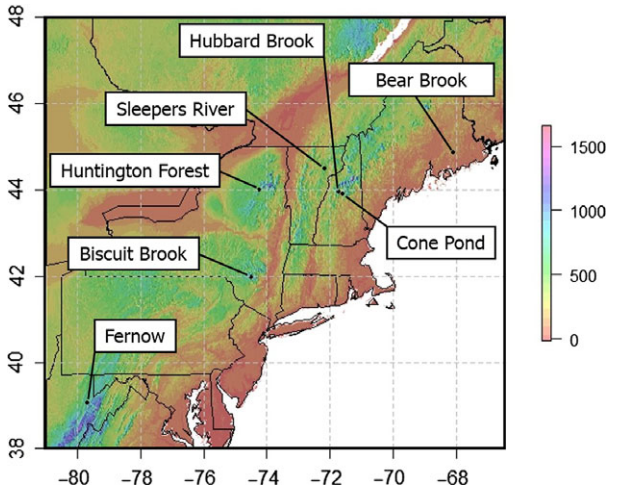


**Fig. 1** Locations of the seven intensive study sites and their elevations in meters.

energy, water, and major elements ($Ca^{2+}$, $Mg^{2+}$, $K^+$, $Na^+$, C, N, P, S, Si, $Al^{3+}$, $Cl^-$, and $F^-$) in forest ecosystems. The model considers major ecosystem processes, including atmospheric deposition, $CO_2$ effects on vegetation, canopy interactions with precipitation, and atmospheric deposition, root uptake, litterfall, soil organic matter dynamics, nitrification, mineral weathering, chemical reactions involving gas, solid and solution phases, and surface water processes (Gbondo-Tugbawa *et al.*, 2001). PnET-BGC has been used to assess the effects of climate change on hydrology (Campbell *et al.*, 2011) and biogeochemistry (Pourmokhtarian *et al.*, 2012) at Hubbard Brook, as well as atmospheric deposition and land disturbance on soil and surface waters in northern forest ecosystems at local and regional scales (Chen & Driscoll, 2004, 2005; Chen *et al.*, 2004; Zhou *et al.*, 2015). One limitation of the PnET-BGC model is the assumption of a homogeneous distribution of vegetation at the watershed scale and constant forest composition during the simulation (i.e., no changes in species assemblages). Therefore, the model does not consider vegetation changes that may occur as climate changes, as well as other factors (e.g., pests, pathogens), which could alter hydrological (e.g., transpiration) and biological (e.g., uptake, growth) processes. Although shifts in dominant tree species are expected to occur slowly in response to changing climate absent major disturbance, the effects might be more pronounced at study sites in forest transition zones (e.g., between northern hardwoods and red spruce-balsam fir forests).

PnET-BGC requires inputs of meteorological data, atmospheric deposition, forest disturbance history, vegetation, soil, and site parameters. Meteorological inputs include a time series of monthly maximum and minimum air temperature (°C), photosynthetically active radiation (PAR; mmol $m^{-2}$ $s^{-1}$), precipitation (cm), and atmospheric $CO_2$ concentration (ppm). Atmospheric deposition includes monthly wet and constant dry to wet ratios of major elements. PnET-BGC uses the dominant forest cover type (i.e., northern hardwood trees, spruce-fir, red oak/red maple, and red pine) and its associated generalized physiological characteristics. Soil information

**Table 1** Location and characteristics of the seven intensive study sites

| Site (Id., region) | Stream | Lat., long. | State | Record length (yrs) | Elevation (m) | Forest cover | Size (ha) | Annual precipitation (cm) | Annual discharge (mm) | Literature |
|---|---|---|---|---|---|---|---|---|---|---|
| Bear Brook (BBWM; NE) | East Bear | 44°52′N, 68°06′W | ME | 20 | 265–475 | Northern Hardwood | 11 | 125 | 920 | Norton *et al.* (1999) |
| Hubbard Brook (HBEF; NE) | WS6 | 43°57′N, 71°44′W | NH | 45 | 550–790 | Northern Hardwood | 13 | 140 | 880 | Likens & Bormann (1995) |
| Cone Pond (CPW; NE) | Inlet | 43°54′N, 71°36′W | NH | 19 | 485–650 | Spruce-Fir | 33 | 128 | 670 | Bailey *et al.* (1995) |
| Sleepers River (SRW; NE) | W-9 | 44°29′N, 72°10′W | VT | 18 | 520–680 | Northern Hardwood | 41 | 132 | 740 | Shanley *et al.* (2002) |
| Huntington Forest (HWF; NE) | Archer Creek | 44°00′N, 74°13′W | NY | 14 | 460–825 | Northern Hardwood | 135 | 121 | 830 | Mitchell *et al.* (2001) |
| Biscuit Brook (BSB; NE) | Biscuit Brook | 41°59′N, 74°30′W | NY | 25 | 620–1125 | Northern Hardwood | 990 | 152 | 970 | Murdoch *et al.* (1998) |
| Fernow (FEF; SE) | WS4 | 39°03′N, 79°41′W | WV | 37 | 750–870 | Central Hardwood | 39 | 146 | 710 | Adams *et al.* (1994) |

includes soil mass per unit area, cation exchange capacity, cation exchange and anion adsorption coefficients, water-holding capacity, element weathering rates, and elemental stoichiometry. Site characteristics include historical land disturbance (e.g., forest harvesting, hurricane, ice storm, fire) as well as latitude, longitude, and elevation (Gbondo-Tugbawa *et al*., 2001; Chen & Driscoll, 2005; Zhai *et al*., 2008). The effects of atmospheric $CO_2$ on vegetation, including response of stomatal conductance and a $CO_2$ fertilization effect on biomass, were implemented by a multilayered submodel of photosynthesis and phenology developed by Ollinger *et al*. (1997, 2002) using a constant ratio of leaf internal to ambient concentration of $CO_2$ ($C_i/C_a$). A detailed description of PnET-BGC is provided by Aber & Driscoll (1997) and Aber *et al*. (1997), and a detailed sensitivity analysis of parameters and state variables is provided by Gbondo-Tugbawa *et al*. (2001) and Pourmokhtarian *et al*. (2012). Model simulations were run on a monthly time step with an initiation period starting at year 1000 to allow for the soil and vegetation pools to reach steady state. Model hydrological outputs include monthly streamflow, transpiration, evaporation, water use efficiency, soil moisture, water stress index (DWater), snow pack, and snow melt. Because the model was run on a monthly time step, it does not capture hydrological variability and processes (e.g. rapid snow melt, intense precipitation event) that occur on a finer time scale (e.g., daily). However, a monthly time step is adequate to investigate the long-term response of watersheds to anticipated changing climate.

The DWater term is a model-calculated estimate of the degree of stomatal closure due to suboptimal water availability. It is an unitless metric of water stress which ranges from 0 (full water stress) to 1 (absence of water stress). Soil water stress (DWater) and actual evapotranspiration are functions of plant water demand and available soil water for each time step of a simulation (monthly for this analysis). If the plant water demand is higher than available soil water for a month, water stress occurs and the value of DWater decreases to <1 (e.g., a DWater value of 0.9 indicates that there is a 10% shortage of available soil water for trees in that month of model simulation). Therefore, if the sum of DWater for all months of an annual simulation is 12, there is no water stress for any month during that year. An annual DWater value <12 indicates that trees experience water stress in some months over an annual simulation. For this analysis, we subtracted mean of simulated DWater values for the reference period (1970–2000) from simulated DWater values for the period of 2070–2100 (Δ DWater). Therefore, more negative Δ DWater values indicate greater water stress of trees compared to the reference period. The DWater index shows the effects of water stress on forest net carbon gain, carbon allocation, and transpiration loss, which is reflected by changes in hydrology.

### *Climate scenarios/downscaling*

To estimate potential changes in climate during the 21st century, we used modeled output from the IPCC AR5 (Flato *et al*., 2013). Four AOGCMs that best represented past trends in precipitation in the region were included in the analysis: the Community Climate System Model version 4 (CCSM4) from the National Center for Atmospheric Research (NCAR; Gent *et al*., 2011); the Hadley Centre Global Environmental Model version 2, Carbon Cycle (HadGEM2-CC) of the Met Office Hadley Centre, United Kingdom (Collins *et al*., 2011); the Model for Interdisciplinary Research on Climate version 5 (MIROC5) of the Center for Climate System Research, Japan (Watanabe *et al*., 2010); and the Meteorological Research Institute Coupled GCM version 3 (MRI-CGCM3) of the Meteorological Research Institute, Tsukuba, Japan (Yukimoto *et al*., 2012). We used the Representative Concentration Pathway scenarios (RCP; Moss *et al*., 2008, 2010) RCP8.5 (Thomson *et al*., 2011) and RCP4.5 (Riahi *et al*., 2011) to represent possible higher and lower emission scenarios, respectively. By the end of the current century (i.e., 2099), atmospheric $CO_2$ concentrations have been projected to reach approximately 936 ppm $CO_2$-equivalent under the RCP8.5 scenario and approximately 538 ppm $CO_2$-equivalent under the RCP4.5 scenario. Detailed descriptions and rationale for these scenarios are provided by Moss *et al*. (2008, 2010), Riahi *et al*. (2011), and Thomson *et al*. (2011). In total, eight climate change scenarios were developed for this study at each site (four AOGCMs each and two emissions scenarios).

Daily coarse resolution maximum and minimum temperature values, precipitation amounts, and solar radiation data from AOGCMs were statistically downscaled and 'trained' (i.e., by developing a relationship between observed climate and historical model output to correct for biases in the climate model (Hayhoe *et al*., 2008)) on measured long-term data from each site using the asynchronous regional regression model (ARRM) approach (Stoner *et al*., 2013). The ARRM method builds on the statistical technique used by Dettinger *et al*. (2004) by assigning quantitative relationships between daily measured and simulated variables that have symmetric distributions. ARRM makes historical measurements and simulations independent of time by ranking them before matching their quantiles using a piecewise regression approach for each of the 12 months individually (Stoner *et al*., 2013). Time independence is an important aspect of this approach as AOGCMs have inherent variability patterns that do not correspond with day-to-day or even year-to-year variability patterns of measured values (Stoner *et al*., 2013).

## Results

### *Future climate projections*

Downscaled AOGCM climate projections for the two emission scenarios for all sites indicate that the increases in average air temperature for the period 2070–2100 would range from 1.2 to 8.5 °C (Table 2, Fig. S1). Note that the errors, biases and uncertainties in downscaling methods and sets of observations used to train the downscaling method have been evaluated in detail by Stoner *et al*. (2013) and Pourmokhtarian *et al*. (2016). For these analyses, mean long-term projections (2070–2100) were compared with measured values for

**Table 2** Summary of projected change in annual air temperature and annual precipitation from statistically downscaled AOGCM output. The value shown for each scenario is the difference between the mean of observed values for the reference period (1970–2000) and the simulation period 2070–2100

| Study Watershed | Climate Variable | 1970–2000* Observed | 2070–2100 CCSM4 RCP 8.5 | CCSM4 RCP 4.5 | HadGEM2-CC RCP 8.5 | HadGEM2-CC RCP 4.5 | MIROC5 RCP 8.5 | MIROC5 RCP 4.5 | MRI-CGCM3 RCP 8.5 | MRI-CGCM3 RCP 4.5 |
|---|---|---|---|---|---|---|---|---|---|---|
| Bear Brook | Temperature (°C) | 6.6 | 4.9 | 2.6 | 6.3 | 4.6 | 8.0 | 4.4 | 4.6 | 2.3 |
| | Annual Precipitation (cm) | 131 | 42.8 | 42.2 | 54.2 | 52.7 | 55.5 | 51.8 | 54.1 | 37.2 |
| Sleepers River* | Temperature (°C) | 4.7 | 4.0 | 1.7 | 6.4 | 4.0 | 6.5 | 3.4 | 3.6 | 1.6 |
| | Annual Precipitation (cm) | 125 | 27.3 | 17.8 | 33.5 | 36.1 | 34.9 | 23.2 | 21.8 | 12.2 |
| Huntington Forest | Temperature (°C) | 4.7 | 5.4 | 3.0 | 7.4 | 4.9 | 8.0 | 4.8 | 4.2 | 2.3 |
| | Annual Precipitation (cm) | 107 | 6.2 | 3.5 | 6.5 | 6.0 | 13.0 | 5.4 | 10.0 | 2.7 |
| Hubbard Brook | Temperature (°C) | 5.7 | 4.8 | 2.5 | 6.6 | 4.4 | 7.2 | 4.1 | 4.1 | 2.0 |
| | Annual Precipitation (cm) | 144 | 23.6 | 19.1 | 24.6 | 26.5 | 30.2 | 21.3 | 22.3 | 15.8 |
| Cone Pond* | Temperature (°C) | 5.7 | 4.8 | 2.5 | 6.6 | 4.4 | 7.3 | 4.1 | 4.2 | 2.1 |
| | Annual Precipitation* (cm) | 127 | 29.7 | 32.3 | 45.9 | 46.0 | 27.3 | 22.7 | 22.0 | 16.3 |
| Biscuit Brook* | Temperature (°C) | 5.3 | 4.6 | 2.3 | 6.6 | 4.5 | 6.9 | 3.9 | 3.8 | 1.9 |
| | Annual Precipitation (cm) | 155 | 29.0 | 26.9 | 56.5 | 36.2 | 52.8 | 44.8 | 39.9 | 18.5 |
| Fernow | Temperature (°C) | 9.4 | 4.9 | 2.5 | 8.5 | 4.0 | 6.5 | 4.0 | 2.7 | 1.2 |
| | Annual Precipitation (cm) | 147 | 14.0 | 2.5 | 3.3 | −5.7 | 22.3 | 16.1 | 33.4 | 9.6 |

*Note that for sites that do not have observed values for the entire period of 1970–2000, observed data for shorter periods are used as described in the Methods section. Sleepers River temperature and precipitation data are from 1991 to 2000; Cone Pond precipitation data are from 1990 to 2000; Biscuit Brook temperature and precipitation data are from 1984 to 2000.

1970–2000 (Sleepers River temperature and precipitation data are from 1991 to 2000, Cone Pond precipitation data are from 1990 to 2000, and Biscuit Brook temperature and precipitation data are from 1984 to 2000). There was a strong negative correlation ($P$ value < 0.05, $r = -0.91$) between measured mean annual air temperature for the period of 1970–2000 and projected percent increases in mean annual temperature for 2070–2100 across all sites and all scenarios (Fig. S2a). Note that removing the FEF from the correlation analysis still yields a negative correlation, but with a slightly higher $P$ value ($P$ value < 0.1, $r = -0.76$). There was a positive correlation ($P$ value = 0.08, $r = 0.70$) between measured mean annual air temperature for the period of 1970–2000 and relative standard deviation (RSD) of projected increases in mean annual temperature for 2070–2100 across all sites and all scenarios (Fig. S2b). However, this relationship is not strong and is largely influenced by the high projected variability for the Fernow Experimental Forest (FEF). The greatest temperature increase was projected by HadGEM2-CC-RCP8.5 for FEF (8.5 °C), while MRI-CGCM3-RCP4.5 showed the smallest temperature increase (1.2 °C) also for FEF, resulting in the greatest variability in projected changes in temperature (RSD = 54.6%) among the sites studied (Fig. S2b). The variability for other sites ranged from 39.1% to 41.3%, with the exception of the Sleepers River Watershed (SRW; RSD = 46.9%). Across all eight climate scenarios, MRI-CGCM3-RCP4.5 and HadGEM2-CC-RCP4.5 showed the highest (RSD = 20.5%) and the lowest (RSD = 7.5%) variability in projected changes in temperature, respectively. The low-emission scenario (RCP4.5) showed higher variability across all sites and AOGCM simulations (Avg. RSD = 15.6%) compared to the high-emission scenario (RCP8.5; Avg. RSD = 11.1%), with the exception of HadGEM2-CC (RSD of RCP8.5 and RCP4.5 are 11.1% and 7.5%, respectively). The average variability of projected increases in temperature for a given climate scenario across all sites was lower compared to average variability of all scenarios (four AOGCMs and two emission trajectories) for a given site.

Precipitation projections were also highly variable for the sites over the period 2070–2100 (Table 2). AOGCMs projections of seasonal patterns in precipitation were

variable across all sites, but in general showed increases over all seasons during the 21st century (Table 3). The magnitude of increases is generally higher under the high-emissions scenario (RCP 8.5) compared to the low-emissions scenario (RCP 4.5). The greatest annual precipitation increase was projected by HadGEM2-CC-RCP8.5 (56.5 cm) for Biscuit Brook (BSB), while at the other extreme, HadGEM2-CC-RCP4.5 showed a decline in projected precipitation for the FEF (5.7 cm) compared to long-term measurements (Table 2, Fig. S3). Among all sites, the FEF showed the greatest variability across different AOGCMs for projected changes in annual precipitation (RSD = 103.6%), while the Bear Brook Watershed in Maine (BBWM) had the lowest variability (RSD = 14.3%). Across all eight climate scenarios, HadGEM2-CC-RCP4.5 and MIROC5-RCP8.5 exhibited the maximum (RSD = 74.9%) and minimum (RSD = 46.2%) variability in projected changes in annual precipitation, respectively. The low-emission scenario (RCP4.5) showed higher variability across all sites and AOGCM simulations (mean RSD = 68.5%) compared to the high-emission scenario (RCP8.5; mean RSD = 53%). The average variability of projected increases in precipitation for a given climate scenario across all study sites was higher than the average variability of all scenarios (four AOGCMs and two emission trajectories) for a given site.

All the sites except the FEF showed a positive significant relationship between AOGCM projections of temperature and precipitation (Fig. 2). The maximum slope of the precipitation response to projected increases in temperature was 6.5 cm $°C^{-1}$ for BSB, while the FEF had a negative slope (−0.45 cm $°C^{-1}$). The slope of the regression between projections of changes in temperature and precipitation was statistically significant ($P < 0.05$) across all sites except for the CPW and FEF. The overall regression line for the relationship between projected changes in precipitation with temperature change for all sites was statistically significant ($P < 0.1$) with a slope of 2.15 cm $°C^{-1}$ ($r^2 = 0.06$). The HBEF had the highest coefficient of determination ($r^2 = 0.78$) between temperature and precipitation followed by BSB ($r^2 = 0.77$), SRW ($r^2 = 0.74$), BBWM ($r^2 = 0.6$), and HWF ($r^2 = 0.52$). The relatively large increase in precipitation in response to increases in temperature for BBWM was likely attributable to the marine influence at this site.

### *Hydrology*

The model simulations of evapotranspiration (ET) showed increases across all sites, AOGCM simulations, and scenarios, although the response was highly variable across sites (Fig. S4a and b). Considering $CO_2$ effects on vegetation decreased annual ET across all sites, AOGCM simulations, and scenarios (Fig. S4a and b). Among all sites, with or without $CO_2$ effects on vegetation, the high-emission scenario (RCP8.5) had a greater increase in projected mean annual ET compared to the low-emission scenario (RCP4.5; Fig. S5). Across all sites, a comparison of ET between high- and low-emission scenarios based on percentage change rather than absolute change showed a similar pattern except for BSB, which had the highest relative change in mean annual ET (Fig. S6). A regression analysis between projected increases in the percentage change in mean annual ET and mean annual temperature showed a significant ($P < 0.05$) positive relationship ($r^2 = 0.21$) across all sites (Fig. 3). Under model simulations with $CO_2$ effects on vegetation, the regression remained significant ($P < 0.05$), with $r^2$ increasing to 0.36. All individual sites except the FEF ($P = 0.14$) and HWF ($P = 0.06$) exhibited a significant positive relationship ($P < 0.05$) between percentage change in mean annual ET and mean annual change in temperature, with the SRW having the strongest relationship ($r^2 = 0.9$), and BSB having the weakest significant relationship ($r^2 = 0.76$). Invoking $CO_2$ effects on vegetation increased the $r^2$ value and decreased the $P$ value for all sites except CPW and SRW, making the regressions of change in evapotranspiration against change in temperature positively significant for nearly all sites. The only exception was the FEF where the relationship was insignificant despite an increase in the $r^2$ value and decrease in $P$ value ($P = 0.07$; Fig. 3).

The model projections of mean annual streamflow were highly variable, ranging from a significant decrease at HWF and FEF to significant increases for the remainder of the sites except for the HBEF that shows both increases and decreases in annual streamflow depending on the scenario and emissions trajectory (Fig. S7a and b). When $CO_2$ effects on vegetation were invoked, streamflow increased under all scenarios and across all sites compared to scenarios without $CO_2$ effects (Fig. S7a and b). A regression analysis between projected change in mean annual simulated streamflow and change in annual precipitation showed a significant ($P < 0.05$) positive relationship ($r^2 = 0.48$) across all sites (Fig. 4a). Under model simulations with $CO_2$ effects on vegetation, the regression remained significant ($P < 0.05$), with $r^2$ slightly decreasing (to 0.46). Across all sites without $CO_2$ effects, only BSB ($r^2 = 0.62$) and CPW ($r^2 = 0.91$) exhibited a significant positive relationship ($P < 0.05$) between projected change in mean annual simulated streamflow and annual precipitation. Invoking $CO_2$ effects made the regression positively significant for BSB, CPW, FEF, and SRW (Fig. 4b). There were no significant differences between

**Table 3** Summary of projected seasonal precipitation (cm) under low- and high-emission scenarios for three periods of 2011–2040, 2041–2070, and 2071–2100

| Study Watershed | Emission Scenario | 1970–2000* | Spring | | | Summer | | | Fall | | | Winter | | |
|---|---|---|---|---|---|---|---|---|---|---|---|---|---|---|
| | | Observed | 2011–2040 | 2041–2070 | 2071–2100 | 2011–2040 | 2041–2070 | 2071–2100 | 2011–2040 | 2041–2070 | 2071–2100 | 2011–2040 | 2041–2070 | 2071–2100 |
| Bear Brook | RCP 4.5 | 131 | 37.4 | 38.0 | 41.2 | 40.7 | 42.1 | 44.1 | 49.1 | 50.5 | 52.4 | 39.0 | 39.8 | 39.7 |
| | RCP 8.5 | | 40.2 | 39.4 | 42.0 | 42.2 | 40.0 | 43.5 | 45.7 | 50.6 | 52.7 | 36.2 | 42.6 | 45.1 |
| Sleepers River* | RCP 4.5 | 125 (1991–2000) | 33.9 | 34.2 | 35.9 | 36.3 | 38.4 | 39.5 | 37.9 | 38.6 | 40.2 | 29.4 | 29.4 | 31.1 |
| | RCP 8.5 | | 34.7 | 35.0 | 37.3 | 39.1 | 39.5 | 38.7 | 37.3 | 42.1 | 42.8 | 29.1 | 32.6 | 35.0 |
| Huntington | RCP 4.5 | 107 | 26.6 | 25.4 | 26.8 | 28.5 | 28.8 | 28.8 | 28.8 | 28.8 | 29.2 | 25.0 | 25.2 | 26.6 |
| Forest | RCP 8.5 | | 26.5 | 26.0 | 28.1 | 29.5 | 29.5 | 27.3 | 27.4 | 30.8 | 31.6 | 24.1 | 27.2 | 28.9 |
| Hubbard | RCP 4.5 | 144 | 36.7 | 37.0 | 39.2 | 40.0 | 40.9 | 42.5 | 41.9 | 42.6 | 44.2 | 36.9 | 36.8 | 38.8 |
| Brook | RCP 8.5 | | 38.3 | 37.4 | 40.8 | 41.7 | 40.0 | 40.7 | 40.6 | 44.1 | 44.7 | 35.1 | 40.7 | 43.1 |
| Cone Pond* | RCP 4.5 | 127 (1990–2000) | 32.3 | 32.7 | 34.9 | 41.4 | 42.4 | 44.4 | 38.3 | 39.1 | 42.2 | 34.2 | 33.9 | 34.8 |
| | RCP 8.5 | | 34.2 | 34.6 | 36.7 | 43.4 | 41.3 | 41.9 | 37.0 | 41.6 | 42.1 | 32.1 | 35.6 | 38.0 |
| Biscuit Brook* | RCP 4.5 | 155 (1984–2000) | 41.7 | 42.4 | 46.6 | 48.8 | 49.4 | 50.4 | 48.8 | 48.2 | 48.3 | 39.4 | 39.5 | 40.9 |
| | RCP 8.5 | | 43.7 | 43.8 | 49.9 | 51.4 | 50.4 | 50.1 | 45.7 | 53.3 | 54.2 | 37.8 | 41.8 | 44.8 |
| Fernow | RCP 4.5 | 147 | 42.7 | 43.4 | 41.2 | 37.2 | 40.3 | 38.4 | 34.6 | 35.3 | 34.3 | 38.7 | 38.5 | 38.9 |
| | RCP 8.5 | | 45.1 | 42.3 | 45.1 | 39.8 | 40.1 | 40.7 | 34.4 | 36.9 | 37.1 | 37.4 | 40.1 | 42.9 |

*Note that for sites that do not have observed values for the entire period of 1970–2000, observed data for a shorter period are used.

 

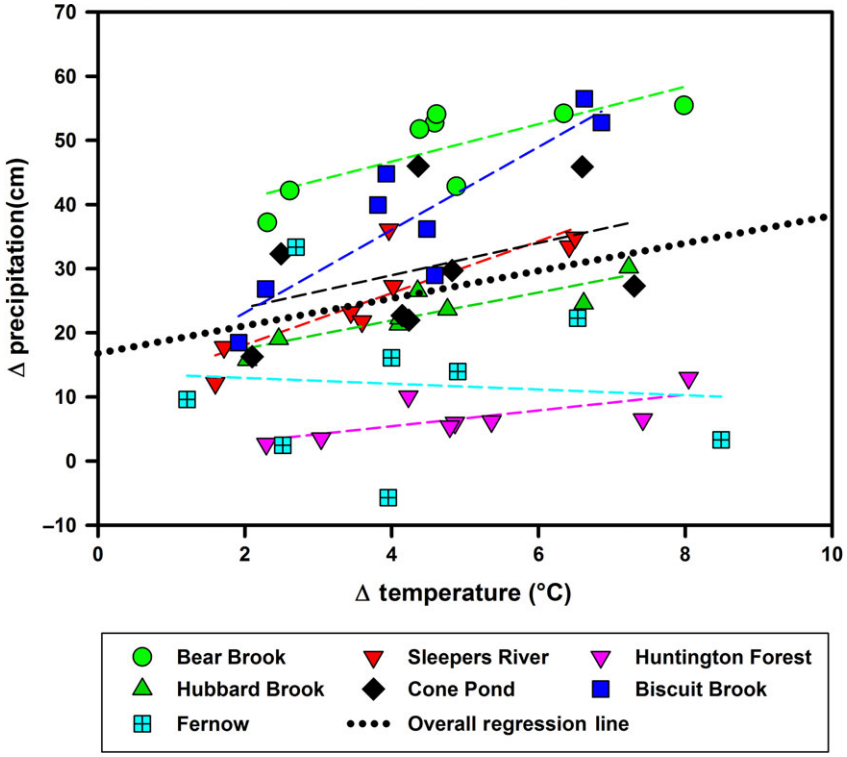


**Fig. 2** Relationships between projected increases in mean annual temperature and annual precipitation from eight climate change scenarios at each site (four AOGCMs each and two emission scenarios) for the period of 2070–2100 compared to the reference period of 1970–2000. The black dotted line shows the overall regression line for all data.

average projected annual changes in streamflow under high (RCP8.5)- and low (RCP4.5)-emissions scenarios for any of the study sites with or without $CO_2$ effects (Fig. S8). A comparison of projected changes in mean annual streamflow across all sites indicated that on average the high-emission scenarios have greater variability across AOGCMs (SD = 68 & 78 mm $yr^{-1}$) than low-emission scenarios (SD = 54 & 62 mm $yr^{-1}$) with and without $CO_2$ effects on vegetation, respectively (Fig. S8).

Based on PnET-BGC model results, climate change was projected to cause substantial long-term shifts in streamflow across all sites (Tables 4 and 5). The extent of these modeled changes depended on the AOGCM used, emission scenario, and site characteristics including location and vegetation. The most notable pattern in streamflow under the two emissions scenarios across all sites was a seasonal shift toward higher winter (January–March) flows (except the FEF under RCP 4.5) and lower spring (April–June) flows. In general, the magnitude of increases and decreases in winter and spring flows, respectively, were higher under the high-emissions scenario (RCP 8.5) compared to the low-emissions scenario (RCP 4.5). Summer (July–September) flows showed a decline over the 21st century across all sites with the exception of CPW under RCP 4.5 and BBWM under both emissions scenarios. Across all sites, fall (October–December) flows were projected to increase, with the exception of HWF and BSB (under RCP 4.5) and FEF (under both emissions scenarios).

Invoking $CO_2$ effects on vegetation increased seasonal streamflow across all sites and emissions scenarios compared to the same period under simulations without $CO_2$ effects. Winter and spring flow patterns remained similar to runs without considering $CO_2$ effects on vegetation, while summer flow patterns were variable, showing decreases, increases, or relatively no change depending on the site and emissions scenarios. Fall flows increased when $CO_2$ effects were included in simulations across all sites and scenarios with the exception of HWF under RCP 4.5, which remained relatively constant, and FEF for which fall flows decreased under both emissions scenarios.

The model projections of water stress index (DWater) indicated that there were significant changes in water deficit for vegetation at all sites under all climate change projections with the exception of the CPW (spruce-fir site) and the FEF under the MRI-CGCM3-RCP4.5 and MRI-CGCM3-RCP8.5 scenarios (Fig. S9a and b). The FEF responses under both high- and

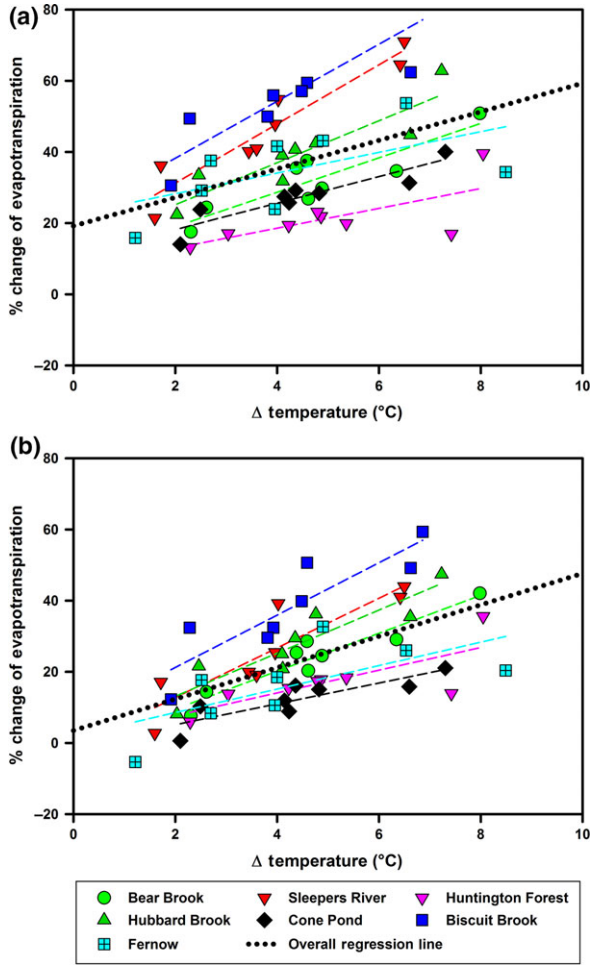


**Fig. 3** Relationships between projected increase in mean annual simulated percentage change in evapotranspiration and change in annual temperature from eight climate change scenarios at each site (four AOGCMs each and two emission scenarios) for the period of 2070–2100 compared with the reference period (1970–2000). The black dotted line shows the overall regression line for all data. Panel (a) shows the results without $CO_2$ effects on vegetation and panel (b) shows the results with $CO_2$ effects.

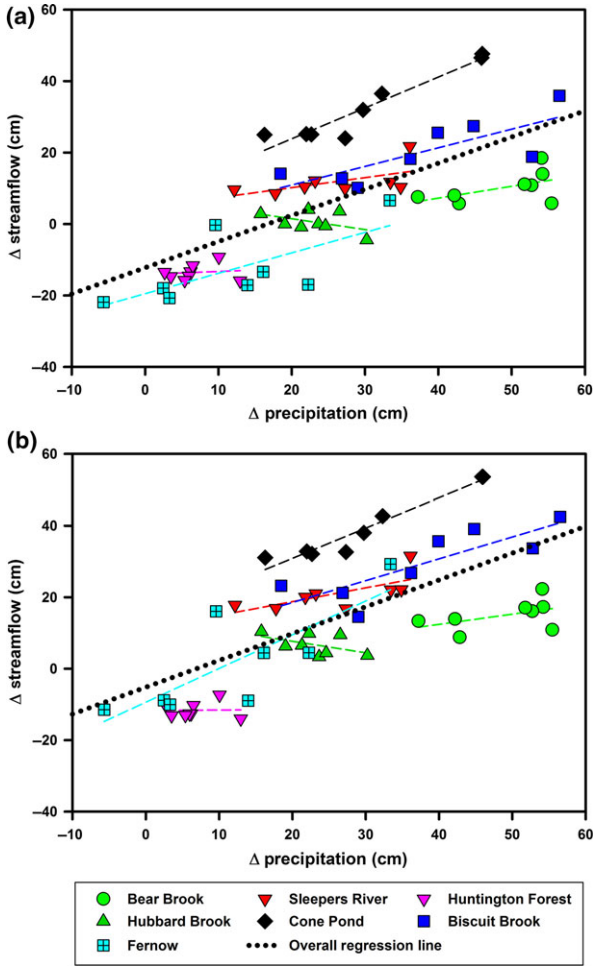


**Fig. 4** Relationships between projected change in mean annual simulated streamflow and change in annual precipitation from eight climate change scenarios at each site (four AOGCMs each and two emission scenarios) for the period of 2070–2100 compared with the reference period (1970–2000). The black dotted line shows the overall regression line for all data. Panel (a) shows the results without $CO_2$ effects on vegetation and panel (b) shows the results with $CO_2$ effects.

low-emission scenarios showed the greatest variability in projected water stress among all study sites (SD = 0.3) and the CPW had the smallest variability (SD = 0.0). Invoking $CO_2$ effects on vegetation alleviated water stress on trees and decreased the drought index under all scenarios and across all sites due to increased WUE (Fig. S9a and b). On average, across all sites, the high-emission scenario (RCP8.5) projected greater water stress (Δ DWater = −0.1 and −0.4 with and without $CO_2$ effects, respectively) with greater variability, due to higher temperature projections, compared to the low-emissions scenario (RCP4.5; Δ DWater = 0.0 and −0.2 with and without $CO_2$ effects, respectively; Fig. S10). A comparison of DWater across all sites based on percentage change showed a similar pattern for values expressed as absolute change (data not shown). When $CO_2$ effects on vegetation were not considered, the HWF and HBEF showed a significant negative ($P < 0.05$) relationship between projected percentage changes in mean annual DWater and mean annual temperature, with the HWF having the strongest significant relationship ($r^2 = 0.93$) and the BSB and SRW having the weakest significant relationship ($P < 0.1$; Fig. 5a). There was no significant relationship between percentage change in mean annual DWater and mean annual temperature for BBWM, CPW, and FEF. For CPW, which is dominated by spruce-fir vegetation, water stress did not change with increasing temperature (Fig. 5a). Model simulations with $CO_2$ effects on vegetation considered showed a significant negative

**Table 4** Summary of projected seasonal streamflow (mm) without invoking $CO_2$ effects on vegetation under low- and high-emission scenarios for three periods of 2011–2040, 2041–2070, and 2071–2100

| Study Watershed | Emission Scenario | 1971–2000* Observed | Spring 2011–2040 | Spring 2041–2070 | Spring 2071–2100 | Summer 2011–2040 | Summer 2041–2070 | Summer 2071–2100 | Fall 2011–2040 | Fall 2041–2070 | Fall 2071–2100 | Winter 2011–2040 | Winter 2041–2070 | Winter 2071–2100 |
|---|---|---|---|---|---|---|---|---|---|---|---|---|---|---|
| Bear Brook* | RCP 4.5 | 922.2 (1990–2000) | 285.2 | 234.5 | 222.6 | 81.8 | 94.1 | 100.0 | 342.9 | 351.1 | 376.1 | 274.8 | 311.4 | 323.7 |
| | RCP 8.5 | | 291.1 | 206.7 | 171.6 | 91.5 | 74.5 | 98.0 | 317.7 | 364.3 | 383.2 | 256.5 | 339.8 | 385.9 |
| Sleepers River* | RCP 4.5 | 755.9 (1992–2000) | 307.5 | 265.5 | 258.3 | 112.0 | 106.1 | 109.4 | 266.9 | 269.2 | 287.3 | 182.5 | 199.5 | 215.8 |
| | RCP 8.5 | | 305.4 | 234.7 | 191.3 | 132.0 | 99.8 | 81.8 | 262.6 | 305.2 | 301.9 | 185.0 | 228.5 | 273.2 |
| Huntington | RCP 4.5 | 698.5 (1999–2009) | 178.5 | 142.6 | 140.2 | 35.2 | 31.7 | 31.7 | 176.2 | 168.3 | 169.1 | 179.8 | 198.7 | 211.9 |
| Forest* | RCP 8.5 | | 172.8 | 125.7 | 116.8 | 39.3 | 33.6 | 31.4 | 164.9 | 186.5 | 181.8 | 181.4 | 216.1 | 243.9 |
| Hubbard Brook | RCP 4.5 | 932.3 | 312.9 | 247.0 | 245.9 | 91.1 | 86.5 | 91.0 | 291.1 | 291.3 | 310.0 | 236.7 | 273.7 | 292.9 |
| | RCP 8.5 | | 310.3 | 220.5 | 178.3 | 103.5 | 76.4 | 77.3 | 277.9 | 307.0 | 310.2 | 232.9 | 303.2 | 357.4 |
| Cone Pond* | RCP 4.5 | 653.2 (1990–2000) | 264.4 | 221.2 | 233.6 | 177.3 | 181.1 | 201.9 | 291.2 | 294.7 | 324.3 | 211.1 | 237.9 | 243.3 |
| | RCP 8.5 | | 266.1 | 220.8 | 194.9 | 196.2 | 166.7 | 173.9 | 280.5 | 319.6 | 324.9 | 206.0 | 250.7 | 296.1 |
| Biscuit Brook* | RCP 4.5 | 947.8 (1984–2000) | 375.9 | 293.4 | 308.1 | 169.3 | 147.7 | 153.3 | 367.1 | 360.0 | 362.5 | 244.5 | 289.4 | 304.5 |
| | RCP 8.5 | | 374.3 | 280.1 | 265.4 | 185.6 | 152.3 | 136.1 | 336.2 | 407.8 | 404.0 | 251.4 | 308.1 | 365.8 |
| Fernow | RCP 4.5 | 670.8 | 135.2 | 104.7 | 97.3 | 42.7 | 45.8 | 41.6 | 139.1 | 118.1 | 95.7 | 324.6 | 314.9 | 306.7 |
| | RCP 8.5 | | 152.5 | 97.3 | 93.4 | 54.7 | 43.2 | 47.5 | 132.8 | 118.2 | 98.5 | 312.3 | 315.4 | 314.2 |

*Note that for sites that do not have observed values for the entire period of 1971–2000, observed data for a shorter period are used.

 

**Table 5** Summary of projected seasonal streamflow (mm) with invoking $CO_2$ effects on vegetation under low- and high-emission scenarios for three periods of 2011–2040, 2041–2070, and 2071–2100

| Study Watershed | Emission Scenario | 1971–2000* Observed | Spring | | | Summer | | | Fall | | | Winter | | |
|---|---|---|---|---|---|---|---|---|---|---|---|---|---|---|
| | | | 2011–2040 | 2041–2070 | 2071–2100 | 2011–2040 | 2041–2070 | 2071–2100 | 2011–2040 | 2041–2070 | 2071–2100 | 2011–2040 | 2041–2070 | 2071–2100 |
| Bear Brook* | RCP 4.5 | 922.2 (1990–2000) | 295.0 | 251.1 | 245.0 | 90.3 | 104.7 | 121.4 | 348.1 | 360.4 | 389.4 | 274.9 | 311.4 | 323.8 |
| | RCP 8.5 | | 303.3 | 228.6 | 186.9 | 100.6 | 88.0 | 109.6 | 324.1 | 377.4 | 393.6 | 256.5 | 340.1 | 386.5 |
| Sleepers River* | RCP 4.5 | 755.9 (1992–2000) | 317.8 | 285.4 | 285.7 | 130.6 | 138.5 | 154.8 | 273.3 | 281.1 | 302.4 | 182.5 | 199.5 | 215.8 |
| | RCP 8.5 | | 317.7 | 265.8 | 223.6 | 151.8 | 145.8 | 122.0 | 270.0 | 323.0 | 324.4 | 185.0 | 228.6 | 273.8 |
| Huntington Forest* | RCP 4.5 | 698.5 (1999–2009) | 182.8 | 147.9 | 148.0 | 37.2 | 33.1 | 37.4 | 180.2 | 175.4 | 179.2 | 179.8 | 198.7 | 211.9 |
| | RCP 8.5 | | 176.6 | 134.0 | 122.2 | 41.6 | 37.8 | 33.3 | 170.0 | 197.5 | 188.9 | 181.4 | 216.3 | 244.1 |
| Hubbard Brook | RCP 4.5 | 932.3 | 322.9 | 265.0 | 269.4 | 102.3 | 104.9 | 121.4 | 296.3 | 302.2 | 323.8 | 236.8 | 273.7 | 292.9 |
| | RCP 8.5 | | 321.8 | 246.0 | 199.4 | 116.2 | 98.7 | 93.1 | 285.2 | 325.4 | 327.2 | 232.9 | 303.5 | 358.5 |
| Cone Pond* | RCP 4.5 | 653.2 (1990–2000) | 272.1 | 237.3 | 254.9 | 194.0 | 209.8 | 237.9 | 293.0 | 299.0 | 329.6 | 211.3 | 238.4 | 244.1 |
| | RCP 8.5 | | 275.7 | 243.2 | 218.7 | 214.9 | 205.5 | 213.5 | 282.8 | 326.9 | 333.1 | 206.2 | 252.1 | 298.1 |
| Biscuit Brook* | RCP 4.5 | 947.8 (1984–2000) | 388.7 | 318.7 | 341.4 | 190.2 | 183.6 | 201.3 | 371.9 | 371.3 | 375.3 | 244.5 | 289.4 | 304.7 |
| | RCP 8.5 | | 389.0 | 315.7 | 299.5 | 208.8 | 195.7 | 169.9 | 342.2 | 423.8 | 422.7 | 251.4 | 308.6 | 366.9 |
| Fernow | RCP 4.5 | 670.8 | 154.9 | 135.3 | 126.3 | 53.7 | 72.6 | 62.5 | 169.1 | 170.2 | 158.1 | 333.4 | 329.1 | 328.4 |
| | RCP 8.5 | | 174.2 | 129.8 | 131.7 | 71.4 | 69.4 | 79.7 | 166.3 | 190.2 | 161.8 | 320.3 | 332.2 | 338.9 |

*Note that for sites that do not have observed values for the entire period of 1971–2000, observed data for a shorter period are used.

 

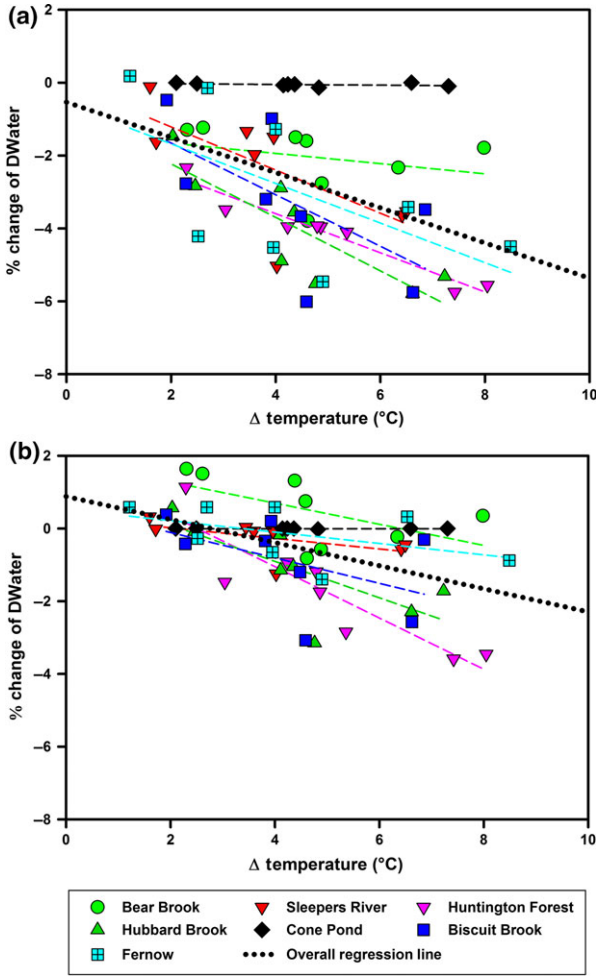


**Fig. 5** Relationships between projected percentage change in mean annual simulated water stress index (DWater) and increase in mean annual temperature from eight climate change scenarios at each site (four AOGCMs each and two emission scenarios) for the period of 2070–2100 compared with the reference period (1970–2000). The black dotted line shows the overall regression line for all data. Panel (a) shows the results without $CO_2$ effects on vegetation and panel (b) shows the results with $CO_2$ effects.

relationship ($P < 0.05$) for BSB ($r^2 = 0.95$), HBEF ($r^2 = 0.53$), and HWF ($r^2 = 0.80$; Fig. 5b). The overall regression analysis between projected percentage changes in mean annual DWater and mean annual temperature showed a significant ($P < 0.05$) negative relationship ($r^2 = 0.23$ and 0.21) across all sites, both with and without $CO_2$ effects, respectively (Fig. 5).

## Discussion

### *Future climate projections*

Projected changes in temperature and precipitation were the main drivers of hydrological responses across all northeastern United States forest sites and were further influenced by vegetation type and response to increases in atmospheric $CO_2$ and soil characteristics (e.g., water-holding capacity). The strong negative correlation between measured mean annual air temperature for the period of 1970–2000 and projected percent increases in mean annual temperature of 2070–2100 across all sites and all scenarios indicates that the relative change in temperature is greater at sites that experience inherently colder temperatures compared to changes at warmer sites. Therefore, the FEF that has the highest measured mean annual temperature (9.4 °C) compared to other sites was projected to experience less relative warming compared to colder sites such as the SRW (4.7 °C) and HWF (6 °C). There was no apparent spatial gradient in projected temperature increases with latitude (with the exception of FEF, which is the most southern site), although, for a given site, projected air temperature increased with increasing global emissions.

No clear spatial pattern in projected changes in precipitation was apparent under future emissions, although FEF and HWF that are the furthest inland compared to other sites showed the smallest projected increases in precipitation. Projections suggest more precipitation during late fall, winter, and early spring and lower precipitation in summer across all sites. We expected that projected increases in precipitation would be greatest at sites with greater ambient precipitation compared to sites with less precipitation. Although there was no statistically significant relationship between measured mean annual precipitation for 1970–2000 and projected increases in precipitation for the period of 2070–2100, sites that currently receive greater precipitation than the average for the study sites were projected to receive greater than average future increases in precipitation. The FEF was an exception to this pattern as it experiences the second highest mean annual precipitation of 1460 mm, after BSB (1750 mm); however, the average projected increase in mean annual precipitation from all climate change scenarios for the FEF was 119 mm, which is the second lowest projected increase among sites (after the HWF). At the extreme, the HadGEM2-CC-RCP4.5 scenario projected a decline in future precipitation at the FEF. On average, the variability of projected increases in precipitation for a given climate scenario (e.g., HadGEM2-CC-RCP4.5) across all study sites was greater than the average variability of all eight scenarios (four AOGCMs and two emission trajectories) for a given site. This pattern indicates that downscaling an AOGCM precipitation projection for a given site using its measured observations decreases the variability of a scenario and therefore uncertainty in precipitation projections at the local scale

(Pourmokhtarian *et al.*, 2016). Although precipitation projections are clearly important, the large interannual variability and uncertainty associated with these projections suggest that regional temperature-driven changes are more homogenous and might be more effectively used as metrics for climate change impact assessments.

### *Hydrology*

Changes in climate could significantly impact forest growth and productivity, which in turn would alter the magnitude and timing of hydrological cycles (Campbell *et al.*, 2009). Our previous study for the HBEF showed that changes in temperature and precipitation control the response of the forest ecosystem water cycle to changing climate (Pourmokhtarian *et al.*, 2012). Therefore, we anticipated that these drivers would be dominant at other regional sites. While some northeastern United States sites did exhibit this response, projections for FEF, HWF, and CPW showed varied hydrological responses of seasonal and annual streamflow, ET, and soil moisture.

The FEF experiences higher annual average air temperatures than other sites and these relatively elevated temperatures are anticipated to increase under future projections. The FEF also shows the greatest variability in projected temperature and precipitation increases across AOGCMs considered, with both increases and decreases in precipitation depending on the climate scenario. Greater variability in projections of temperature and precipitation at the FEF resulted in more variable projected increases in annual ET compared to other sites (no statistically significant relationship between projected changes in ET and air temperature). The FEF is the only study site with central hardwood forest cover. Since this site was not glaciated during the Pleistocene, soils are much older and highly weathered and therefore contain more clay and the highest water-holding capacity (WHC; 30 cm) among study sites (12 cm for other sites). In the PnET-BGC model, WHC is defined as available water for plants and depends on soil texture and rooting depth. The higher WHC at the FEF mitigates the effects of higher temperatures to some extent by allowing for greater water storage to supply plant transpiration demand during the extended growing season.

Similar to what was observed at the FEF, the limited response of ET at the HWF to increases in air temperature was due to a lack of available water for transpiration during the growing season because of minimal projected precipitation increases. HWF has the lowest projected increase in precipitation of any of the study sites despite the similarity among temperature projections. Diminished precipitation during the extended growing season increases water stress on trees and decreases the photosynthetic rate, which causes a decrease in ET. Invoking $CO_2$ effects on vegetation decreases projected increases in ET due to increased WUE, resulting in the greatest benefit to sites, like HWF and FEF, which are anticipated to experience the most severe water stress under future climate conditions. FEF and HWF are the most inland sites investigated and showed the lowest projected increase in precipitation. Furthermore, they have different climatic conditions, vegetation (central hardwoods and northern hardwoods, respectively), and WHC (30 and 12 cm, respectively). These differences in site characteristics are largely responsible for the varied hydrological responses at these sites compared with the other study sites.

The weak response of ET to future increases in temperature at the CPW is likely due to the different forest cover type (spruce-fir). The spruce-fir forest has a lower optimum temperature (20 °C) for photosynthesis than northern hardwoods (24 °C; Aber & Federer, 1992), and increases in temperature above the optimum temperature that are projected for the CPW may cause temperature stress on vegetation and a decline in photosynthesis and forest productivity, which leads to lower ET. Climate projections for the CPW do not predict water stress. Therefore, spruce-fir watersheds will likely experience temperature stress before water stress occurs under future climate conditions. It has been shown that even in the absence of water stress, spruce stands respond to increased vapor pressure deficit (VPD) by partial stomatal closure (Running & Coughlan, 1988), therefore lowering ET losses (Aber & Federer, 1992). Lastly, the spruce-fir forest at the CPW has a lower photosynthetic capacity due to lower foliar N and therefore lower transpiration demand that can eliminate water stress compared to northern hardwoods (Aber & Federer, 1992). Therefore, projected increase in ET for the coniferous forest of the CPW is largely driven by temperature and a lengthening of the growing season rather than by changes in precipitation since trees do not show evidence of water stress under future climate projections. These results are consistent with previous model runs by Ollinger *et al.* (2009) for another conifer site at the Howland Forest in Maine. Invoking $CO_2$ effects on vegetation during the growing season lowered ET at CPW due to increased WUE, similar to the response at other sites.

PnET-BGC calculates ET and water stress for each month as a function of available soil water and plant water demand. Aber & Federer (1992) derived a relationship for the response of tree photosynthesis to changes in temperature, providing parameter values for different forest cover types ranging from temperate

to boreal based on the literature. They defined a multiplier (coefficient) between 0 and 1 to depict the effect of temperature on gross photosynthesis, which is a parabolic function that varies with forest cover type. They determined that the optimum temperature for gross photosynthesis is 24 °C and 20 °C for northern hardwood trees and spruce-fir, respectively (Aber & Federer, 1992; Aber *et al.*, 1995; Ollinger *et al.*, 2009). They also characterized foliar respiration as a function of gross photosynthesis, which increases with temperature as a $Q_{10}$ factor of 2 (Aber & Federer, 1992; Ollinger *et al.*, 2009). The $Q_{10}$ is a measure of the temperature dependency of a rate process (e.g., change in foliar respiration if temperature increases by 10 °C). A projected lengthening of the growing season and associated increases in ET due to higher temperatures could limit available soil water and ultimately lead to water stress to plants, despite projected increases in precipitation. Model simulations under lower emissions scenarios for the northeastern United States where hydrology is strongly influenced by snow melt (except the more southerly FEF) indicate that projected increases in annual ET largely occur during the late spring, summer, and early fall due to the extended growing season. Under the higher emissions scenarios, the increases in ET extend into the shoulder seasons causing a greater increase in annual ET. Across all sites except the FEF, projected increases in ET during the shoulder seasons are due to a decline in snow pack associated with higher temperature and increases in the fraction of precipitation occurring as rain vs. snow. Increases in ET increase water stress on plants and decrease streamflow during summer. Model simulations that included $CO_2$ effects on vegetation showed lower rates of ET due to decreases in stomatal conductance and increased WUE, which is inversely correlated with VPD (Ollinger *et al.*, 2002, 2009). Therefore, if northern hardwood forests respond to increasing atmospheric $CO_2$ similarly to the response of vegetation in the free-air $CO_2$ enrichment (FACE) experiments from which these relationships were based (Curtis *et al.*, 1995; Ellsworth *et al.*, 1995; Lewis *et al.*, 1996; Curtis & Wang, 1998; Saxe *et al.*, 1998; Ellsworth, 1999; Ainsworth & Long, 2005), they will be able to mitigate the effects of increases in temperature to some extent.

The projections of water stress across all sites and under all climate change scenarios, although highly variable, suggest a general trend of drier conditions during the growing season in the future, despite projected increases in precipitation. This trend is driven by decreases in mean monthly soil moisture during summer and early fall as a result of increased ET and is reflected in lower summer discharge from these watersheds. The high variability in water stress projections is consistent with high variability in increased precipitation projections across sites, AOGCM projections and scenarios. Summer drought is largely driven by depletion of soil water by ET, exhausting the short-term water supply. As the soil water-deficit increases, tree productivity declines, which in turn decouples soil–vegetation processes and decreases nutrient retention. Even short-term water stress on plants during the growing season can hamper productivity and carbon and nitrogen sequestration and disrupt element cycling.

Model projections of future climate scenarios suggest a seasonal shift in streamflow toward greater discharge during fall and winter and lower spring and summer flows across all sites. Projections also show that spring high flows will occur earlier in the year. At sites with colder climates (e.g., HWF, SRW, HBEF, CPW, BSB, and BBWM), the snow pack will develop later in the season and melt earlier in the spring. These changes in seasonal discharge are due to the diminished role of snow pack and the extended growing season, coupled with the projected increases in precipitation during winter and decreases in summer.

These projected changes in hydrology have important implications for future water management in the northeastern United States and could impact local economies and businesses that depend on recreational activities that are reliant on snow and streamflow. Also, the prospect of warmer summers poses a significant risk to forest productivity and the services provided by these ecosystems. Four of the seven study sites (BBWM, SRW, CPW, and BSB) showed significant increases in projected mean annual streamflow, which was further enhanced when $CO_2$ effects on vegetation were included in simulations, causing decreased ET. In contrast, at the HWF and FEF, projections of mean annual streamflow showed significant declines due to smaller projected increases in precipitation which could cause summer drought and put pressure on water supplies and resources. Finally, at the HBEF, the projected response is highly variable, including increases and decreases in mean annual streamflow depending on the climate change scenario. This level of complexity in the hydrological response of watersheds to changing climate will challenge our ability to respond and adapt to this critical dimension of global change.

Through this study, new insights are provided into how climate change is manifested differently across an array of forested ecosystems with a range of biophysical characteristics. We compared and contrasted the effects of climate change on hydrological responses at seven forested watersheds in the northeastern United States, using a suite of climate projections. Projections indicate that all watersheds will experience significant

increases in ET under future climate change due to warmer temperatures and an extended growing season. Model projections for sites where snow is currently prevalent indicated that the extent of snow pack accumulation will diminish substantially or disappear by the end of the 21st century. Model simulations also suggest that under climate change, northern hardwood forests will experience more frequent and higher intensity drought and water stress during the longer growing season. In contrast, watersheds dominated by spruce-fir (CPW) may show greater susceptibility to temperature stress due to the lower optimum temperature for photosynthesis of conifers compared to hardwoods. The streamflow projections are highly variable across sites with some showing significant increases in annual water yield, while water yield decreases at others. Major factors causing the varied hydrological responses across the study region are variability in projected increases in precipitation, coupled with differences in forest cover and site characteristics (location, soil water-holding capacity). The varied streamflow responses pose a challenge to policymakers and water resource and forest managers. The complexities of the streamflow response to future climate scenarios are particularly important for developing adaptation strategies for flood mitigation in the region for the decades ahead.

Considering the dynamic nature of climate change over both time and space, it is challenging to generalize the long-term climatic shifts across forest watersheds in the northeastern United States. Nevertheless, comparing and contrasting an array of watersheds with a wide range of characteristics provides important insights on the potential range of responses of these diverse ecosystems. Vegetation, soil water-holding capacity, and location are important factors that influence hydrological responses to a changing climate, some of which lend themselves to human intervention as we improve the understanding of these relationships. The close linkages between climate change and vegetation are expected to result in complex patterns across these sites, which could ultimately alter the structure and function of these forests and the services they provide.

## Acknowledgements

The authors would like to thank an anonymous reviewer for providing helpful comments that improved this manuscript. We would also like to thank Colin Fuss and Andrew B. Reinmann for their constructive feedback on earlier drafts of the manuscript. Funding for this study was provided by the Environmental Protection Agency through the STAR program, the USDA Northeastern States Research Cooperative, and the National Science Foundation (NSF) through the Long Term Ecological Research (LTER) program. This manuscript is a contribution of the Hubbard Brook Ecosystem Study. Hubbard Brook is part of the LTER network, which is supported by the NSF. The Hubbard Brook Experimental Forest is operated and maintained by the USDA Forest Service, Northern Research Station, Newtown Square, PA. The data for the Huntington Forest have been provided with funding from NYSERDA (New York State Energy Research Development Authority). The Bear Brook Watershed in Maine is partially supported by the National Science Foundation Long Term Research in Environmental Biology (LTREB) program (DEB 1119709). Watershed research on the Fernow Experimental Forest is supported in part by the National Science Foundation Long Term Research in Environmental Biology (LTREB) program (DEB 1019522), and by the USDA Forest Service. The Sleepers River Watershed in Vermont is supported by USGS Water, Energy, and Biogeochemical Budgets (WEBB) program of the Climate and Land Use Change Mission Area. The Biscuit Brook Watershed is supported by the Long-Term Monitoring Program of the US Environmental Protection Agency's Clean Air Markets Division.

## References

Aber JD, Driscoll CT (1997) Effects of land use, climate variation, and N deposition on N cycling and C storage in northern hardwood forests. *Global Biogeochemical Cycles*, **11**, 639–648.

Aber JD, Federer CA (1992) A generalized, lumped-parameter model of photosynthesis, evapotranspiration and net primary production in temperate and boreal forest ecosystems. *Oecologia*, **92**, 463–474.

Aber JD, Ollinger SV, Federer CA *et al.* (1995) Predicting the effects of climate change on water yield and forest production in the northeastern United States. *Climate Research*, **5**, 207–222.

Aber JD, Ollinger SV, Driscoll CT (1997) Modeling nitrogen saturation in forest ecosystems in response to land use and atmospheric deposition. *Ecological Modelling*, **101**, 61–78.

Adams MB, Kochenderfer JN, Wood F, Angradi TR, Edwards P (1994) *Forty years of hydrometeorological data from the Fernow Experimental Forest, West Virginia*. US Department of Agriculture, Forest Service, Northeastern Forest Experiment Station.

Ainsworth EA, Long SP (2005) What have we learned from 15 years of free-air $CO_2$ enrichment (FACE)? A meta-analytic review of the responses of photosynthesis, canopy properties and plant production to rising $CO_2$. *New Phytologist*, **165**, 351–371.

Bailey SW, Driscoll CT, Hornbeck JW (1995) Acid-base chemistry and aluminum transport in an acidic watershed and pond in New Hampshire. *Biogeochemistry*, **28**, 69–91.

Campbell JL, Rustad LE, Boyer EW *et al.* (2009) Consequences of climate change for biogeochemical cycling in forests of northeastern North America. *Canadian Journal of Forest Research*, **39**, 264–284.

Campbell JL, Driscoll CT, Pourmokhtarian A, Hayhoe K (2011) Streamflow responses to past and projected future changes in climate at the Hubbard Brook Experimental Forest, New Hampshire, United States. *Water Resources Research*, **47**, 15.

Chen L, Driscoll CT (2004) Modeling the response of soil and surface waters in the Adirondack and Catskill regions of New York to changes in atmospheric deposition and historical land disturbance. *Atmospheric Environment*, **38**, 4099–4109.

Chen L, Driscoll CT (2005) A two-layer model to simulate variations in surface water chemistry draining a northern forest watershed. *Water Resources Research*, **41**, 8.

Chen L, Driscoll CT, Gbondo-Tugbawa S, Mitchell MJ, Murdoch PS (2004) The application of an integrated biogeochemical model (PnET-BGC) to five forested watersheds in the Adirondack and Catskill regions of New York. *Hydrological Processes*, **18**, 2631–2650.

Collins WJ, Bellouin N, Doutriaux-Boucher M *et al.* (2011) Development and evaluation of an Earth-System model – HadGEM2. *Geoscientific Model Development*, **4**, 1051–1075.

Comer G, Zimmermann R (1968) Low-flow and basin characteristics of two streams in northern Vermont. *Journal of Hydrology*, **7**, 98–108.

Curtis PS, Wang X (1998) A meta-analysis of elevated $CO_2$ effects on woody plant mass, form, and physiology. *Oecologia*, **113**, 299–313.

Curtis PS, Vogel CS, Pregitzer KS, Zak DR, Teeri JA (1995) Interacting effects of soil fertility and atmospheric $CO_2$ on leaf area growth and carbon gain physiology in Populus × euramericana (Dode) Guinier. *New Phytologist*, **129**, 253–263.

Demaria EMC, Palmer RN, Roundy JK (2016) Regional climate change projections of streamflow characteristics in the Northeast and Midwest U.S. *Journal of Hydrology: Regional Studies*, **5**, 309–323.

Dettinger MD, Cayan DR, Meyer MK, Jeton AE (2004) Simulated hydrologic responses to climate variations and change in the Merced, Carson, and American River basins, Sierra Nevada, California, 1900–2099. *Climatic Change*, **62**, 283–317.

Ellsworth DS (1999) $CO_2$ enrichment in a maturing pine forest: are $CO_2$ exchange and water status in the canopy affected? *Plant, Cell and Environment*, **22**, 461–472.

Ellsworth DS, Oren R, Huang C, Phillips N, Hendrey GR (1995) Leaf and canopy responses to elevated $CO_2$ in a pine forest under free-air $CO_2$ enrichment. *Oecologia*, **104**, 139–146.

Fan F, Bradley RS, Rawlins MA (2014) Climate change in the northeastern US: regional climate model validation and climate change projections. *Climate Dynamics*, **43**, 145–161.

Fernandez IJ, Rustad LE, Norton SA, Kahl JS, Cosby BJ (2003) Experimental acidification causes soil base-cation depletion at the bear brook watershed in Maine. *Soil Science Society of America Journal*, **67**, 1909–1919.

Fernandez IJ, Karem JE, Norton SA, Rustad LE (2007) *Temperature, soil moisture, and streamflow at The Bear Brook Watershed in Maine (BBWM)*. Maine Agricultural and Forest Experiment Station. *Technical Bulletin*, **196**.

Flato G, Marotzke J, Abiodun B, *et al*. (2013) Evaluation of climate models. In: *Climate Change 2013: The Physical Science Basis*. Contribution of Working Group I to the Fifth Assessment Report of the Intergovernmental Panel on Climate Change (eds Stocker TF, Qin D, Plattner G-K, Tignor M, Allen SK, Boschung J, Nauels A, Xia Y, Bex V, Midgley PM), Cambridge University Press, Cambridge, UK.

Gbondo-Tugbawa SS, Driscoll CT, Aber JD, Likens GE (2001) Evaluation of an integrated biogeochemical model (PnET-BGC) at a northern hardwood forest ecosystem. *Water Resources Research*, **37**, 1057–1070.

Gent PR, Danabasoglu G, Donner LJ *et al*. (2011) The community climate system model version 4. *Journal of Climate*, **24**, 4973–4991.

Hayhoe K, Wake CP, Huntington TG *et al*. (2007) Past and future changes in climate and hydrological indicators in the US Northeast. *Climate Dynamics*, **28**, 381–407.

Hayhoe K, Wake C, Anderson B *et al*. (2008) Regional climate change projections for the northeast USA. *Mitigation and Adaptation Strategies for Global Change*, **13**, 425–436.

Johnson CE, Driscoll CT, Siccama TG, Likens GE (2000) Element fluxes and landscape position in a northern hardwood forest watershed ecosystem. *Ecosystems*, **3**, 159–184.

Lewis JD, Tissue DT, Strain BR (1996) Seasonal response of photosynthesis to elevated $CO_2$ in loblolly pine (*Pinus taeda* L.) over two growing seasons. *Global Change Biology*, **2**, 103–114.

Likens GE, Bormann FH (1995) *Biogeochemistry: Of a Forested Ecosystem*. Springer-Verlag, New York, NY, USA.

Matonse AH, Pierson DC, Frei A *et al*. (2011) Effects of changes in snow pattern and the timing of runoff on NYC water supply system. *Hydrological Processes*, **25**, 3278–3288.

Matonse AH, Pierson DC, Frei A, Zion MS, Anandhi A, Schneiderman E, Wright B (2012) Investigating the impact of climate change on New York City's primary water supply. *Climatic Change*, **116**, 437–456.

Melillo JM, Richmond TC, Yohe GW (2014) *Climate Change Impacts in the United States: The Third National Climate Assessment*. U.S. Global Change Research Program, 841 pp. doi:10.7930/J0Z31WJ2.

Mitchell MJ, McHale PJ, Inamdar S, Raynal DJ (2001) Role of within-lake processes and hydrobiogeochemical changes over 16 years in a watershed in the Adirondack Mountains of New York State, USA. *Hydrological Processes*, **15**, 1951–1965.

Moss R, Babiker M, Brinkman S *et al*. (2008) Towards new scenarios for analysis of emissions, climate change, impacts, and response strategies: IPCC Expert Meeting Report, 19–21 September 2007. Noordwijkerhout, The Netherlands, 155.

Moss RH, Edmonds JA, Hibbard KA *et al*. (2010) The next generation of scenarios for climate change research and assessment. *Nature*, **463**, 747–756.

Murdoch PS, Burns DA, Lawrence GB (1998) Relation of climate change to the acidification of surface waters by nitrogen deposition. *Environmental Science & Technology*, **32**, 1642–1647.

NECIA (2006) *Climate Change in the U.S. Northeast. A Report of the Northeast Climate Impacts Assessment*. UCS Publications, Cambridge, MA, USA.

Norton S, Kahl J, Fernandez I *et al*. (1999) The Bear Brook Watershed, Maine (BBWM), USA. *Environmental Monitoring and Assessment*, **55**, 7–51.

Ollinger SV, Aber JD, Reich PB (1997) Simulating ozone effects on forest productivity: interactions among leaf-, canopy-, and stand-level processes. *Ecological Applications*, **7**, 1237–1251.

Ollinger SV, Aber JD, Reich PB, Freuder RJ (2002) Interactive effects of nitrogen deposition, tropospheric ozone, elevated $CO_2$ and land use history on the carbon dynamics of northern hardwood forests. *Global Change Biology*, **8**, 545–562.

Ollinger SV, Goodale CL, Hayhoe K, Jenkins JP (2009) Potential effects of climate change and rising $CO_2$ on ecosystem processes in northeastern U.S. forests. *Mitigation and Adaptation Strategies for Global Change*, **14**, 101–106.

Pourmokhtarian A, Driscoll CT, Campbell JL, Hayhoe K (2012) Modeling potential hydrochemical responses to climate change and increasing $CO_2$ at the Hubbard Brook Experimental Forest using a dynamic biogeochemical model (PnET-BGC). *Water Resources Research*, **48**, W07514.

Pourmokhtarian A, Driscoll CT, Campbell JL, Hayhoe K, Stoner AMK (2016) The effects of climate downscaling technique and observational data set on modeled ecological responses. *Ecological Applications*, **26**, 1321–1337.

Riahi K, Rao S, Krey V *et al*. (2011) RCP 8.5—A scenario of comparatively high greenhouse gas emissions. *Climatic Change*, **109**, 33–57.

Running SW, Coughlan JC (1988) A general model of forest ecosystem processes for regional applications I. Hydrologic balance, canopy gas exchange and primary production processes. *Ecological Modelling*, **42**, 125–154.

Saxe H, Ellsworth DS, Heath J (1998) Tree and forest functioning in an enriched $CO_2$ atmosphere. *New Phytologist*, **139**, 395–436.

Shanley JB, Kendall C, Smith TE, Wolock DM, McDonnell JJ (2002) Controls on old and new water contributions to stream flow at some nested catchments in Vermont, USA. *Hydrological Processes*, **16**, 589–609.

Shepard JP, Mitchell MJ, Scott TJ, Zhang YM, Raynal DJ (1989) Measurements of wet and dry deposition in a Northern Hardwood forest. *Water, Air, and Soil pollution*, **48**, 225–238.

Stewart IT, Cayan DR, Dettinger MD (2005) Changes toward earlier streamflow timing across western North America. *Journal of Climate*, **18**, 1136–1155.

Stoner AMK, Hayhoe K, Yang X, Wuebbles DJ (2013) An asynchronous regional regression model for statistical downscaling of daily climate variables. *International Journal of Climatology*, **33**, 2473–2494.

Thomson AM, Calvin KV, Smith SJ *et al*. (2011) RCP4.5: a pathway for stabilization of radiative forcing by 2100. *Climatic Change*, **109**, 77–94.

Thorne J, Anderson J, Horiuchi K (1988) Cation cycling in a base-poor and base-rich northern hardwood forest ecosystem. *Journal of Environmental Quality*, **17**, 95–101.

Watanabe M, Suzuki T, O'ishi R *et al*. (2010) Improved climate simulation by MIROC5: mean states, variability, and climate sensitivity. *Journal of Climate*, **23**, 6312–6335.

Yukimoto S, Adachi Y, Hosaka M (2012) A new global climate model of the Meteorological Research Institute: MRI-CGCM3: model description and basic performance (special issue on recent development on climate models and future climate projections). *Journal of the Meteorological Society of Japan*, **90**, 23–64.

Zhai J, Driscoll CT, Sullivan TJ, Cosby BJ (2008) Regional application of the PnET-BGC model to assess historical acidification of Adirondack lakes. *Water Resources Research*, **44**, 9.

Zhou Q, Driscoll CT, Sullivan TJ, Pourmokhtarian A (2015) Factors influencing critical and target loads for the acidification of lake–watersheds in the Adirondack region of New York. *Biogeochemistry*, **124**, 353–369.

## Supporting Information

Additional Supporting Information may be found in the online version of this article:

**Appendix S1.** Site descriptions.
**Figure S1.** Projected changes in mean annual air temperature from statistically downscaled AOGCM output for study watersheds for individual AOGCM simulations under different emission scenarios.
**Figure S2.** (a) Relationship between projected percentage increases in mean annual temperature from eight climate change scenarios at each site (four AOGCMs each and two emissions scenarios) for the period of 2070–2100 (Fig. S1) compared to measured mean annual temperature for the reference period of 1970–2000. (b) Relationship between relative standard deviation of projected increases in mean annual temperature from eight climate change scenarios at each site (four AOGCMs each and two emissions scenarios) for the period of 2070–2100 (Fig. S1) compared to measured mean annual temperature for the reference period of 1970–2000. The black dotted line shows the overall regression line for all sites.
**Figure S3.** Projected changes in mean annual precipitation from statistically downscaled AOGCM output for study watersheds for individual AOGCM simulations under different emission scenarios.
**Figure S4.** Projected changes in mean annual evapotranspiration from PnET-BGC output for study watersheds for individual AOGCM simulations under different emission scenarios.
**Figure S5**. Projected changes in mean annual evapotranspiration under high (RCP8.5) and low (RCP4.5) emissions scenarios with and without $CO_2$ effects on vegetation for study watersheds.
**Figure S6.** Projected percentage changes in mean annual evapotranspiration under high (RCP8.5) and low (RCP4.5) emissions scenarios with and without $CO_2$ effects on vegetation for study watersheds.
**Figure S7.** Projected changes in mean annual streamflow from PnET-BGC output under high (RCP8.5) and low (RCP4.5) emissions scenarios with and without $CO_2$ effects on vegetation for study watersheds.
**Figure S8.** Average projected changes in mean annual streamflow under high (RCP8.5) and low (RCP4.5) emissions scenarios with and without $CO_2$ effects on vegetation for study watersheds.
**Figure S9.** Projected changes in mean annual water stress index (DWater) from PnET-BGC output for study watersheds for individual AOGCM simulations under different emission scenarios.
**Figure S10.** Projected changes in mean annual water stress index (DWater) under high (RCP8.5) and low (RCP4.5) emissions scenarios with and without $CO_2$ effects on vegetation for the study watersheds.